Non-Markovian activated rate processes: Comparison of current theories with numerical simulation data[a)]

John E. Straub, Michal Borkovec, and Bruce J. Berne
Department of Chemistry, Columbia University, New York, New York 10027

(Received 25 September 1985; accepted 1 November 1985)

We calculate the barrier crossing rate constants for a Brownian particle in a double well potential experiencing a non-Markovian friction kernel using a full stochastic simulation. We compare the simulation results with recently proposed interpolation formulas which are based on the Grote–Hynes theory and the energy diffusion mechanism. We find that such formulas can fail by orders of magnitude in a physically interesting regime. Slow activation in an effective dynamic double well potential is probably responsible for the deviations observed.

I. INTRODUCTION

Liquid state reactions are often described by the generalized Langevin equation[1–5]

$$\ddot{x} = -\frac{\partial U(x)}{\partial x} - \int_0^t dt'\, \zeta(t-t')\dot{x}(t') + R(t)\,, \quad (1)$$

where the reaction coordinate of unit mass $x(t)$ moves in a double well potential $U(x)$, experiences a friction kernel $\zeta(t)$ and a random force $R(t)$ which originates from the thermal motion of the bath coordinates. The random force $R(t)$ satisfies the second fluctuation–dissipation theorem

$$\langle R(0)R(t)\rangle = (1/\beta)\zeta(|t|)\,, \quad (2)$$

where $\beta = 1/k_B T$.

Kramers[6] treated this problem in the Markovian limit, i.e., where $\zeta(t) = \gamma\delta(t)$ and showed that the rate constant for barrier crossing first increases with the damping γ, reaches a maximum (below the transition state value) and then decreases as $1/\gamma$. This behavior can be understood as originating from two different mechanisms. First, in the underdamped regime energy activation is rate limiting and is responsible for the initial rise. In the overdamped regime spatial diffusion across the barrier region becomes rate limiting and causes the rate constant to decrease. Various connection formulas have been proposed to predict the rate constant for arbitrary damping.[1,3,4,7] Let us mention that the maximum of the rate constant as a function of the damping has recently been observed experimentally.[8]

Because the solvent has a finite correlation time there has been considerable interest in redoing Kramers' calculation with a frequency dependent friction constant. As in the Kramers' treatment various approximations must be invoked to solve this problem. The underdamped regime can again be treated using the energy diffusion equation.[2] The overdamped regime can be treated by similar methods used in the Markovian case.[1,3,5] In the high viscosity regime this theory predicts rate constants which are often much larger than one would obtain in applying the Markovian Kramers' theory. Such non-Markovian theories have been used to explain the experimentally observed slow decrease of the rate constant with increasing viscosity.[9] Connection formulas were also proposed to obtain the overall rate constant in the non-Markovian case.[4,10]

Given the importance of this problem in chemical physics we have studied the validity of these ideas by comparing theoretical predictions with full stochastic simulations. The rapid absorbing boundary method for evaluating the reactive flux makes such calculations of rate constants possible.[11] The simulation data reveal striking deficiencies in the predictions based on the above theories which have been partly reported in a brief letter.[12] Here we discuss the more complete data. Our results lead to the conclusion that in the regime of large viscosity and long correlation times all available theories severely overestimate the rate constant for a single degree of freedom in a double well potential for any physically interesting barrier height. This behavior can be attributed to slow relaxation in an effective dynamic double well potential.

II. THEORETICAL MODELS

For convenience we briefly summarize the available theories for the calculation of rate constants. As a specific illustration let us consider a particle moving in a piecewise harmonic symmetric double well potential[4,13] $U(x)$, with barrier energy Q, well frequency ω_0, and barrier frequency ω_B, and experiencing a simple exponential friction kernel $\zeta(t)$ with Laplace transform

$$\hat{\zeta}(s) = \frac{\gamma}{1+\tau_c s}\,; \quad \tau_c = \alpha\gamma\,, \quad (3)$$

where γ is the static friction (usually assumed to be proportional to the viscosity) and τ_c is the correlation time. The frequency dependent part of the Zwanzig–Bixon hydrodynamic friction kernel[14] which was applied to explain reaction rates in solution[9] is well approximated by Eq. (3) when one takes $\tau_c = \alpha\gamma$ at constant α. This is because the viscoelastic relaxation time is proportional to the viscosity where the proportionality constant α is essentially the inverse of the infinite frequency shear modulus G_∞. We prefer to consider γ and α as the parametrization of the friction kernel. We also use the dimensionless quantity $\alpha^* = \alpha\omega_B^2$.

Since the overall rate constant never exceeds the transition state value

$$k_{TST} = [(\omega_0/(2\pi)]e^{-\beta Q}\,, \quad (4)$$

we report rate constants normalized by this quantity.

[a)] This research was supported by grants from NSF and NIH.

 0021-9606/86/031788-07$02.10

In the underdamped regime the rate limiting step is energy activation which is described by the energy diffusion mechanism, with the rate constant[1-5]

$$k_{\mathrm{ED}} = \frac{1}{2}\left[\int_0^Q dE\, \frac{e^{\beta E}\omega(E)}{D(E)} \int_0^E dE'\, \frac{e^{-\beta E'}}{\omega(E')}\right]^{-1}, \quad (5)$$

where $\omega(E)$ is the frequency at given energy E and

$$D(E) = \frac{1}{\beta}\int_0^\infty dt\, \zeta(t)\langle v(0)v(t)\rangle_E \quad (6)$$

is the energy diffusion coefficient. The microcanonical velocity correlation function $\langle v(0)v(t)\rangle_E$ is to be evaluated for the undamped motion at fixed energy E. The factor 1/2 in Eq. (5) arises because there is equal probability for trapping in each well once the particle oscillates above the barrier threshold.[4,15] For high barriers Eq. (5) can be approximated accurately [i.e., up to terms of $O(e^{-\beta Q})$ compared with unity] by[1,5]

$$k_{\mathrm{ED}} = \frac{\beta}{2\omega_0}\left[\int_{E_0}^Q dE\, \frac{e^{\beta E}\omega(E)}{D(E)}\right]^{-1}, \quad (7)$$

where E_0 is chosen to be on the order of a few k_BT (k_{ED} is independent of the precise value of E_0). The rate constant can be obtained by integrating Eq. (7) numerically. The energy diffusion coefficient is evaluated by expanding $\langle v(0)v(t)\rangle_E$ in a Fourier series.[2] The use of the expression

$$k_{\mathrm{ED}} \simeq \mathrm{Re}\,\zeta(-i\omega_0)\,\frac{\beta Q}{2}e^{-\beta Q} \quad (8)$$

which is obtained by evaluating Eq. (7) approximately requires some caution. Using our friction kernel Eq. (3) we have checked Eq. (8) against Eq. (7) and found that Eq. (8) is a good approximation only if $\omega_B \gg \omega_0$ since in this limit a large part of the potential is a parabolic well. In the opposite limit Eq. (8) is only qualitatively correct and should not be used. This is completely consistent with the more detailed discussion in Ref. 2. As a function of the damping γ the rate constant k_{ED} increases proportionally with γ for small γ like the Kramers' Markovian result. However, as γ becomes larger the correlation time $\tau_c = \alpha\gamma$ increases so much that k_{ED} goes through a maximum and for large γ decreases like $1/\gamma$. Some representative graphs showing this behavior are given by the broken line in Fig. 1.

Before we consider the intermediate and overdamped regime for the general non-Markovian case ($\alpha > 0$) let us focus on the Markovian Kramers case ($\alpha = 0$). Consider first the high damping limit (γ large) where spatial diffusion becomes the rate limiting step so that the rate constant is given by[16]

$$k_{\mathrm{SD}} = \frac{1}{\beta\gamma}\left[\int_{-a}^{a} dx\, e^{\beta U(x)} \int_{-\infty}^{x} dx' e^{-\beta U(x')}\right]^{-1}, \quad (9)$$

where a is the position of the minimum of the symmetric potential $U(x)$. For deep wells one obtains up to exponentially small terms of $O(e^{-\beta Q})$ the result

$$k_{\mathrm{SD}} = \frac{\omega_0}{\gamma}\left(\frac{1}{2\pi\beta}\right)^{1/2}\left[\int_{-a}^{a} dx\, e^{\beta U(x)}\right]^{-1}. \quad (10)$$

This is evaluated for the piecewise parabolic potential $U(x)$ most conveniently by numerical integration. The limiting behavior for large barrier energies ($\beta Q \gg 1$) is easily understood. The main contribution to the integral comes from the barrier region where the potential is well approximated by an inverted parabola and the rate constant is as obtained by Kramers[6]:

$$k_{\mathrm{SD}} \sim k_{\mathrm{TST}}\,(\omega_B/\gamma)\,. \quad (11)$$

However, if we consider the limit $\omega_B \gg \omega_0$ (sharp barrier) at a constant barrier height βQ the contribution from the barrier becomes negligible and the rate constant approaches the result for a cusped barrier

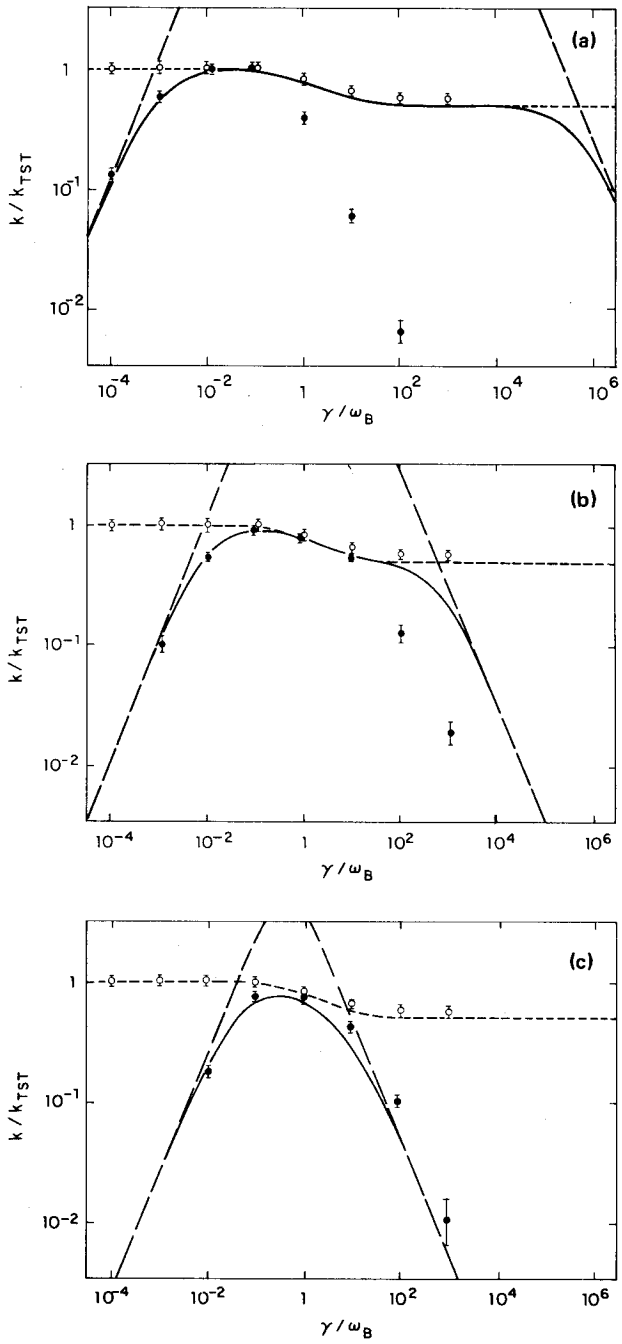

FIG. 1. Rate constants as a function of the static friction for $\beta Q = 20$ and $\alpha^* = 4/3$ for different frequency ratios (a) $\omega_B/\omega_0 = 20$, (b) $\omega_B/\omega_0 = 2$, and (c) $\omega_B/\omega_0 = 0.2$. The simulation data with error bars are represented by dots: (●) on the full double well potential and (○) on the inverted parabola only. The theoretical predictions are represented by lines: Energy diffusion Eq. (7) (– –), Grote–Hynes theory Eq. (13) (- - -), and the interpolation formula Eq. (16) (—).

$$k_{SD} \sim k_{TST}(\omega_0/\gamma)(\pi\beta Q)^{1/2} . \quad (12)$$

Therefore one has to be careful in using Eq. (11) since it can differ substantially from Eq. (10) even for quite high barriers.

Unfortunately, we known of no analog of Eq. (9) for an arbitrary time dependent friction kernel. However, Grote and Hynes[1] initiated the study of the Kramers problem for the case of arbitrary friction where the potential is approximated by an inverted parabola. In this case the rate constant k for crossing the barrier is given by[1,3,5]

$$k_{GH} = k_{TST}(\lambda/\omega_B) , \quad (13)$$

where λ is the largest positive root of the Grote–Hynes relation

$$\lambda^2 + \lambda\hat{\zeta}(\lambda) = \omega_B^2 \quad (14)$$

and $\hat{\zeta}(s)$ is the Laplace transform of the time dependent friction kernel $\zeta(t)$.

For our friction kernel Eq. (3) the Grote–Hynes relation is readily solved numerically. The limiting behavior is again easily understood.[17] For small γ the rate constant k_{GH} approaches k_{TST}. For large γ and vanishing correlation time ($\alpha = 0$) the rate constant reduces to Eq. (11). For large γ and finite correlation times ($\alpha > 0$) two cases have to be distinguished. First, for $\alpha^* < 1 (\alpha^* = \alpha\omega_B^2)$ the rate constant k_{GH} is proportional to $1/\gamma$ for large γ. For $\alpha^* > 1$ however k_{GH} levels off at a constant value for large γ. For $\alpha^* = 4/3$ for example $k_{GH}/k_{TST} \to 1/2$. Such behavior is shown by the dashed curve in Fig. 1. This change in qualitative behavior at $\alpha^* = 1$ can be understood by considering a dynamic confining effective potential with a harmonic frequency $1/\alpha$ which has to be added to the bare potential barrier.[17] For $\alpha^* < 1$ the total effective potential imprisons the particle at the barrier top and the particle must wait until the effective potential relaxes. In this case the rate constant is strongly reduced for large γ as in the Markovian Kramers case. For $\alpha^* > 1$ the total effective potential only renormalizes the frequency of the barrier. In this case the particle can leave the barrier region without any hindrance and the rate constant does not decrease much below the transition state value. We return to this point in Sec. IV.

One is of course interested in the rate constant for arbitrary damping. Let us focus first on the Markovian case ($\alpha = 0$) where the rate constant is well approximated by[11,18]

$$k^{-1} \simeq k_{ED}^{-1} + k_{TST}^{-1} + k_{SD}^{-1} . \quad (15)$$

If the barrier is high enough this expression is close to the more sophisticated formulas[1,4,7] which—roughly speaking—replace in Eq. (15) k_{SD} from Eq. (10) by the asymptotic result Eq. (11). However Eq. (15) is much simpler to use and more accurate if the result from Eq. (10) differs significantly from Eq. (11). This difference can be substantial even for fairly high barriers. For the non-Markovian case it has been proposed that the rate constant k for arbitrary damping and correlation times should be well approximated by[1,3,5,10]

$$k^{-1} \simeq k_{ED}^{-1} + k_{GH}^{-1} \quad (16)$$

or similar formulas.[4] Note that for small α (meaning small correlation times τ_c) and high enough barriers this expression yields rate constants very close to Eq. (15). This is because the two last terms of Eq. (15) represent the simplest Pade approximant for k_{GH}. In Fig. 1 we show representative plots.

III. SIMULATION RESULTS

Given the importance of these ideas in the modern theory of liquid state reactions it is appropriate to compare them with computer simulations and thereby test their validity. We study the exponential friction model, Eq. (3), for a particle in a symmetric piecewise harmonic double well potential described in the beginning of Sec. II.

To study this problem numerically we consider the following set of stochastic differential equations[20]:

$$\begin{aligned} \dot{x} &= v , \\ \dot{v} &= -(\partial U/\partial x) + z , \\ \dot{z} &= -(1/\alpha)v - [1/(\alpha\gamma)]z + \xi , \end{aligned} \quad (17)$$

where the Gaussian noise $\xi(t)$ has correlation function

$$\langle \xi(0)\xi(t) \rangle = [2/(\alpha^2\beta\gamma)]\delta(t) . \quad (18)$$

The elimination of the z variable yields (after an initial transient decay on the time scale of $\alpha\gamma$) Eq. (1) with the proper random force $R(t)$ and friction kernel Eq. (3). Numerical integration of Eq. (17) is achieved using an Adams–Moulton predictor–corrector algorithm.[19] The random force is kept constant during each integration step h which imples that ξ has a finite variance.[11] The integration step h must be chosen small enough that the quantities of interest do not change. Too large an h can cause spurious results. The rate constant is determined using the rapid absorbing boundary version[11] of the reactive flux method.[13] The initial value of x is at the barrier maximum (the transition state), v is sampled from $v \exp(-\beta v^2/2)$ and z from the equilibrium distribution[20] $\exp(-\alpha\beta z^2/2)$. It is crucial to realize that for large γ the trajectories have to be followed for very long times until one reaches the plateau in the reactive flux. Note that only by using the rapid absorbing boundary method[11] were we able to make an accurate determination of the rate constants in this regime (i.e., where $k/k_{TST} \ll 1$). A typical calculation of one rate constant involved the average of 1000 trajectories and required from several minutes up to a few hours on a FPS-164 Attached Processor. The determination of the error bars for the reactive flux is described in the Appendix. All the results of the calculations are displayed in Table I. The calculation procedure has been checked in several ways: First we have calculated rate constants in a regime where energy diffusion or spatial diffusion are so slow that they will be rate limiting. The corresponding values of the rate constants must agree with the theoretical values obtained from Eq. (7) or (10), respectively. As can be seen in Table I the agreement is indeed excellent. A second check involved the calculation of a full reactive flux in the regime of large damping and large correlation times. The result displayed in Table I shows satisfactory agreement with the results obtained from the absorbing boundary method. A third check involved running trajectories just on the bare inverted parabola. In this case the Grote–Hynes theory should be exact[1,3]

TABLE I. Rate constants from simulations in a double well potential for different parameter values. The error bars represent 95% confidence intervals.

βQ	ω_B/ω_0	γ/ω_B	$\omega_B^2\alpha$	k/k_{TST}	k/k_{TST}
20	0.2	0.01	4/3	0.176 ± 0.020	
20	0.2	0.1	4/3	0.753 ± 0.034	
20	0.2	1	4/3	0.745 ± 0.048	
20	0.2	10	4/3	0.439 ± 0.032	
20	0.2	100	4/3	0.103 ± 0.015	
20	0.2	1000	4/3	0.010 ± 0.005	
20	2	0.1	4/3	0.953 ± 0.028	
20	2	1	4/3	0.779 ± 0.047	
20	2	10	4/3	0.536 ± 0.049	
20	2	100	4/3	0.126 ± 0.024	
				0.088 ± 0.018[a]	
20	2	1000	4/3	0.018 ± 0.004	
100	2	1000	4/3	0.064 ± 0.008	
1000	2	1000	4/3	0.379 ± 0.021	
20	20	0.0001	4/3	0.127 ± 0.017	0.119[b]
20	20	0.001	4/3	0.549 ± 0.034	
20	20	0.01	4/3	0.992 ± 0.014	
20	20	0.1	4/3	0.996 ± 0.011	
20	20	1	4/3	0.366 ± 0.042	
20	20	10	4/3	0.056 ± 0.006	
20	20	100	4/3	0.006 ± 0.002	
20	2	1	0.001	0.609 ± 0.035	
20	2	10	0.001	0.106 ± 0.015	
20	20	10	0.01	0.036 ± 0.009	0.037[c]
20	20	0.1	0.01	0.929 ± 0.043	
20	0.2	100	0.1	0.014 ± 0.010	
20	0.2	100	0.5	0.053 ± 0.020	
20	2	300	0.5	0.014 ± 0.010	
20	0.2	100	0.7	0.107 ± 0.028	
20	0.2	300	1	0.049 ± 0.019	
20	2	100	2.5	0.128 ± 0.031	
20	2	1000	2.5	0.025 ± 0.010	
20	2	300	10	0.024 ± 0.014	
20	0.2	0.1	25	0.132 ± 0.018	0.145[b]
20	0.2	1	25	0.022 ± 0.007[b]	0.016[b]
20	20	10	25	0.141 ± 0.033	
20	20	100	25	0.016 ± 0.006	

[a] Full reactive flux calculation.
[b] Theoretical prediction of the rate constant from Eq. (7) in the energy diffusion region.
[c] From Eq. (10) in the spatial diffusion region.

and the simulations should agree with Eq. (13). This is also the case as can be seen in Figs. 1(a)–1(c).

A first set of simulations was run by varying the ratio of the well to barrier frequency at constant $\alpha^* = 4/3$ and $\beta Q = 20$. The results are summarized in Fig. 1. At low γ one can see the rise of the rate constant due to energy diffusion which is shown as the broken line. As one increases γ the rate constant decreases as $1/\gamma$ due to the energy diffusion mechanism. At intermediate γ one would expect the Grote–Hynes relation (shown as dashed line) to be rate limiting over a wide range of γ. Surprisingly, however, this does not happen and the rate constant decreases much sooner. Note the extreme deviations in the case of a sharp barrier ($\omega_B/\omega_0 = 20$) shown in Fig. 1(a). In all cases considered we observed empirically that to high accuracy the decrease of the rate constant is proportional to $1/\gamma$ as one would expect from energy diffusion but with a much smaller proportionality coefficient. We studied this coefficient f defined by

$$k/k_{TST} \simeq (\omega_B/\gamma) f \qquad (19)$$

for large γ with f independent of γ. The simulation results for f as a function of α^* are summarized in Fig. 2 for different ω_B/ω_0. For energy diffusion f turns out to be proportional to $1/\alpha^2$ for large γ and the factor f can be explicitly evaluated from Eqs. (7), (6), and (3) and is shown as a broken line in Fig. 2. Furthermore the Grote-Hynes relation gives $f = 1/(1-\alpha^*)$ if $\alpha^* < 1 (\alpha^* = \alpha\omega_B^2)$. This is shown by the dashed line in Fig. 2. The value of f at $\alpha = 0$ is given by Eq. (9). Note that in the case where one can make a saddle point approximation to Eq. (9) [cf. Eq. (10)] $f = 1$ (for $\alpha = 0$). The factor f predicted by the interpolation formula Eq. (16) is not shown in Fig. 2 since it is very close to the Grote–Hynes relation for $\alpha^* < 1$ and to the energy diffusion result for $\alpha^* > 1$. One can see that the simulation results approach the theoretical laws for small and large α^*. However there is a region for $\alpha^* \gtrsim 1$ which exhibits a behavior not predicted by any of the theories discussed. These deviations are most pronounced in the case of a sharp barrier. For example for $\omega_B/\omega_0 = 20$ and $\alpha^* = 4/3$ Eq. (16) would predict a limiting slope which is five orders of magnitude too large.

To gain a better understanding of where the problems arise consider the potential with fixed $\beta Q = 20$ and $\omega_B/\omega_0 = 2$ at arbitrary damping γ and correlation time τ_c. We plot contours of equal k/k_{TST} in Fig. 3. The heavy lines are the rate constants obtained by approximate interpolation of our simulation data and are thus only semiquantitative. Dashed lines are the predictions of Eq. (16). The straight line represents the cut through Fig. 3 at $\alpha^* = 4/3$ which is shown in Fig. 1(b). Note that the energy diffusion mechanism is rate limiting in the left as well as in the upper portion of Fig. 3. On the other hand, spatial diffusion is rate limiting in the lower right corner. The shaded region is where Eq. (16) overestimates severely the rate constant. These prob-

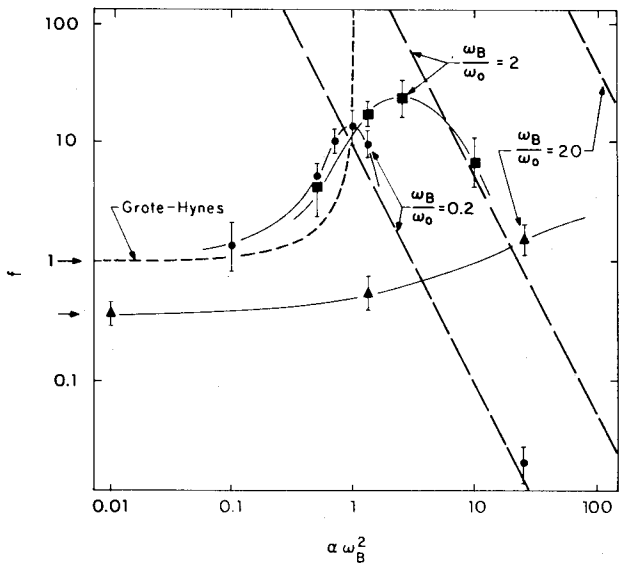

FIG. 2. The limiting slope for the rate constant which seems to be proportional to $1/\gamma$ for large γ for $\beta Q = 20$ and different ratios of ω_B/ω_0. The energy diffusion mechanism Eq. (5) is represented by (– –), the results of spatial diffusion at $\alpha = 0$ by arrows (→), and the prediction of Grote–Hynes relation Eq. (13) (---). The simulation data are presented for $\omega_B/\omega_0 = 0.2$ (●), $\omega_B/\omega_0 = 2$ (■), and $\omega_B/\omega_0 = 20$ (▲). The line connecting them is for an eye guide only.

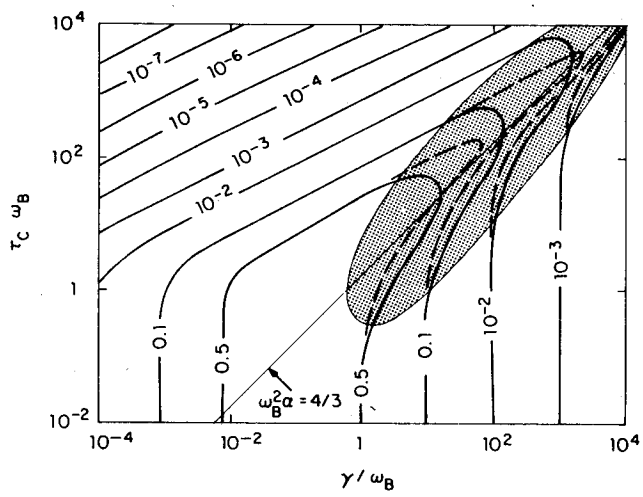

FIG. 3. Plot of equal rate constants for different damping γ and correlation time τ_C for $\beta Q = 20$ and $\omega_B/\omega_0 = 2$. The approximate interpolation of the simulation data (—) and the prediction of the interpolation formula Eq. (16) (– –). The shaded region shows the parameter values where one finds most serious disagreement. The diagonal line represents the cut shown in Fig. 1(b) at $\alpha^* = 4/3$.

lems appear to arise if $\alpha^* > 1$ and if at the same time the energy diffusion mechanism is not rate limiting. If we decrease ω_B/ω_0 at constant βQ (flatter barrier) the energy diffusion mechanism becomes slower. The shaded region where Eq. (16) overestimates the rate constant shrinks rapidly since the slow energy diffusion covers up this region completely. Note that previous numerical results[4] which show good agreement with Eq. (16) were performed for small ω_B/ω_0 where no problems are expected. However, if we increase ω_B/ω_0 at constant βQ (sharp barrier) the shaded region grows rapidly to an enormous size thus making the application of the interpolation formula Eq. (16) nugatory.

We have made some exploratory calculations of the dependence on βQ of the rate constant in the shaded region of Fig. 3 for the case $\omega_B/\omega_0 = 2$, $\alpha^* = 4/3$, and $\gamma/\omega_B = 1000$. From Table I it can be seen that as βQ is increased from 20 to 1000 the rate constant seems to approach the expected value of 0.5 given by Grote–Hynes theory Eq. (13).

IV. INTERPRETATION

To understand the reason for the serious failure of the interpolation formula, Eq. (16), let us first consider some sample trajectories and phase plots shown in Fig. 4. In each case the trajectory is started at the barrier top and followed until trapped for a long period in either well as would be done in a full reactive flux calculation. On the left in Fig. 4 the position of the particle is shown as a function of time. On the right the corresponding phase plot shows the same trajectory in position and velocity space. For comparison in Fig. 4(a) a typical trajectory in the underdamped energy diffusion regime is plotted. One can see that the particle oscillates, almost freely, above the barrier threshold until it is trapped in the upper well. In Fig. 4(b) a trajectory in the overdamped spatial diffusion regime is shown. The particle performs a Brownian motion in position space. From the phase plot one can see the fast relaxation of the velocity in this case. In the case where Grote–Hynes theory applies [Fig. 4(c)] the trajectory is immediately trapped as it leaves the barrier region. However in the case when there are large deviations from Eq. (16) one can see very clearly [in Fig. 4(d)] that as soon as the particle reaches the anharmonic region of the potential it turns around and recrosses. Such rapid recrossings are not treated by the interpolation formula Eq. (16) and lead to a dramatic decrease in the rate constant. From Figs. 4(c) and 4(d) it appears that the particle moves in an effective dynamic double well potential whose spatial extension is much smaller than the full double well. The form of the effective potential is readily derived explicitly. Since we are in the regime of large correlation time we can approximate the kernel $\zeta(t)$ in Eq. (1) by its initial value $\zeta(0) = 1/$

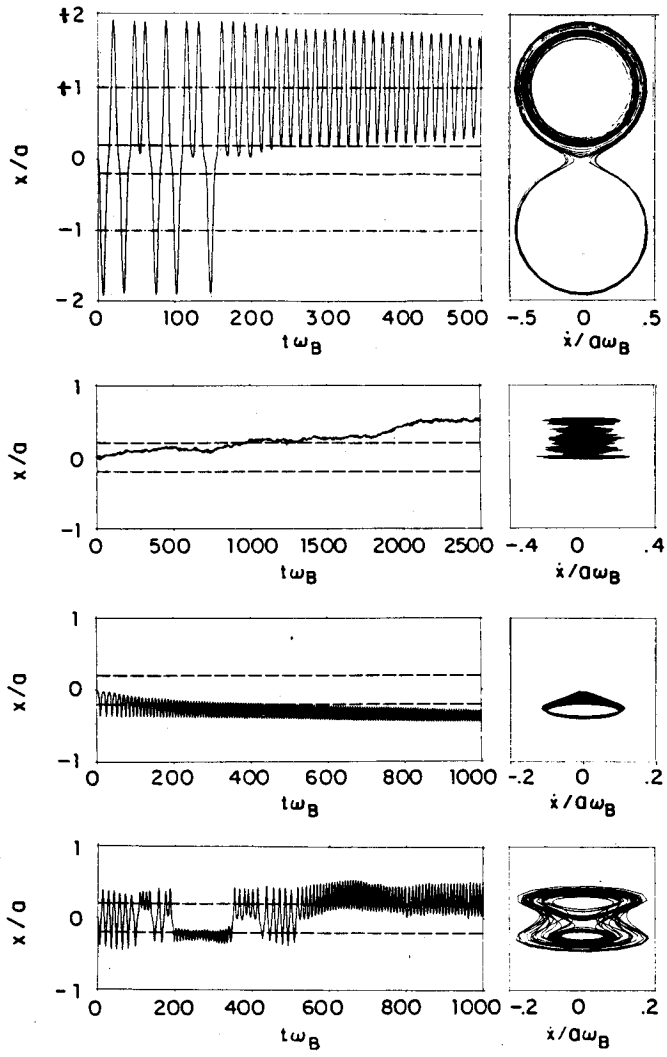

FIG. 4. Sample trajectories shown as position as a function of time (left) and as a plot in position and velocity spaces. The barrier lies at $x = 0$ and the distance from the barrier to the position of the minimum of the well is a (–·–) and the joining point of the parabolas is $a/5$ (– –). (a) Energy diffusion region ($\alpha^* = 4/3$, $\gamma/\omega_B = 0.01$, $\beta Q = 20$, $\omega_B/\omega_0 = 2$). (b) Spatial diffusion region ($\alpha^* = 0.01$, $\gamma/\omega_B = 100$, $\beta Q = 20$, $\omega_B/\omega_0 = 2$). (c) Region where Eq. (16) applies ($\alpha^* = 4/3$, $\gamma/\omega_B = 1000$, $\beta Q = 1000$, $\omega_B/\omega_0 = 2$). (d) Region where Eq. (16) fails ($\alpha^* = 4/3$, $\gamma/\omega_B = 1000$, $\beta Q = 20$, $\omega_B/\omega_0 = 2$).

α and the time integral can be performed with the initial condition at the barrier $x(0) = 0$. This gives a dynamic correction to the force which can be derived from an effective potential

$$U_{\text{eff}}(x) = U(x) + [1/(2\alpha)]x^2 . \tag{20}$$

If we consider the barrier region ($x \to 0$) we obtain[17]

$$U_{\text{eff}}(x) \sim [(1/\alpha^*) - 1](\omega_B^2/2)x^2 + \cdots , \tag{21}$$

where $\alpha^* = \alpha\omega_B^2$. For $\alpha^* < 1$ the effective potential is confining and imprisons the particle for the length of a correlation time. For $\alpha^* > 1$ the barrier remains repelling but has only a renomalized frequency. However, if we plot this effective potential (see Fig. 5) for $\alpha^* < 1$ the effective potential is confining but for $\alpha^* > 1$ it is an effective double well potential which deepens as we increase α and approaches the bare potential for large α. If we start a particle on the top of the barrier and it becomes trapped with a high probability on one side of the effective double well potential [as in Fig. 4(c)] Grote–Hynes theory will apply. If on the other hand the particle is not trapped easily on one side of the effective double well potential and recrosses many times before trapping [as in Fig. 4(d)] one has to expect that Eq. (16) in theory will severely overestimate the rate constant. This idea can be quantified by assuming that the loss of energy is responsible for the trapping in the metastable well. The energy diffusion rate constant Eq. (5) in this effective double well potential is able to predict the simulation data shown in Fig. 2 for not too small α within an order of magnitude. Obviously this idea can work only semiquantitatively since the effective potential is not static but changes in time. Nevertheless this appears to be a good point of departure for developing a complete theory of this effect.

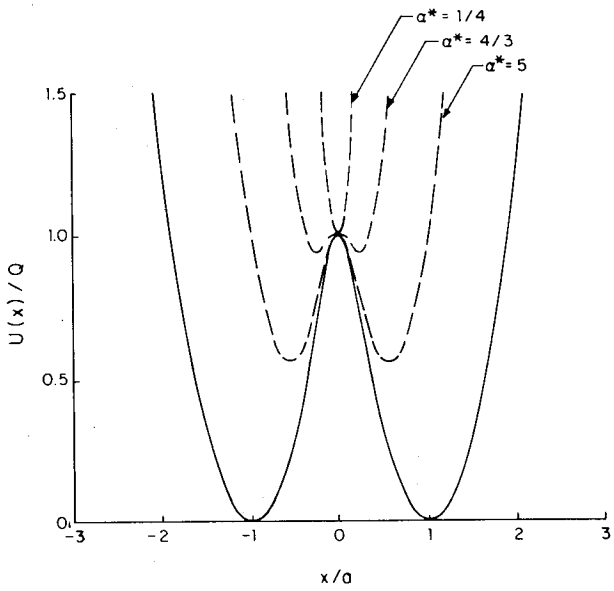

FIG. 5. Effective dynamic potential Eq. (20) for different α^*'s (– –). The bare potential which coincides with the effective potential for $\alpha \to \infty$ is drawn for comparison (—).

V. CONCLUSION

We have performed numerical simulations of a Brownian particle experiencing frequency dependent friction. We evaluated the barrier crossing rate constant of a double well potential. We have confirmed that in the Markovian case the simulation data are accurately described for any damping by a simple connection formula Eq. (15) for all barrier heights of physical interest (e.g., $\beta Q \gtrsim 5$).

For a non-Markovian bath however, connection formulas such as Eq. (16) exhibit serious problems for similar barrier heights. The present theories can overestimate the simulation data by orders of magnitude in the high damping (i.e., zero frequency friction) and large correlation time regime. Without being able to determine the f factor defined in Eq. (19) it seems impossible to construct connection formulas which are as powerful as, e.g., Eq. (15) in the Markovian case. We find that the particle moves in a dynamic effective double well potential (see Fig. 5). The slow energy activation in this effective double well potential can become rate limiting and is probably responsible for the deviations observed.

Very recently Hänggi[5] suggested a criterion for the validity of the Grote–Hynes relation which is based on the analysis of the second eigenvalue contributing to the motion on the top of the barrier. To apply Grote–Hynes theory safely the criterion requires that $\bar{\gamma} > \bar{\omega}$ where $\bar{\gamma}$ is the renormalized damping and $\bar{\omega}$ is the renormalized barrier frequency.[3,5] These two quantities are easily evaluated for the present system. One finds that the Grote–Hynes relation is safely applicable for small α and large γ. For larger values of α the criterion is most severely violated for small and large γ. Our simulations show that Grote–Hynes theory indeed works well for large γ and small α and applies for larger values of α at intermediate γ. However, Grote–Hynes theory might still be applicable where the criterion is not satisfied. We observe such behavior for $\alpha = 4/3$ at large βQ for example (where the criterion is not met for any γ) and Grote–Hynes theory still applies for some intermediate γ's.

There is substantial experimental evidence that rate constants for chemical isomerization reactions[9,21] and recombination reactions[8] in liquids often decrease more slowly with the viscosity η than η^{-1}. This fact was recently explained using the Grote–Hynes relation and the Zwanzig–Bixon hydrodynamic friction.[14] Also molecular dynamics data were used to obtain the frequency dependent friction.[22] In both cases it is simple to estimate the quantity $\alpha^* = \omega_B^2 \tau_c / \gamma$. If $\alpha^* > 1$ we are in the region where the Grote–Hynes theory can severely overestimate true rate constants. Taking a typical barrier frequency of $10^{-13}\ \text{s}^{-1}$ it turns out that α^* can very roughly between 1 and 10. This means that the regime of interest for chemical reactions in liquids lies just where Eq. (16) severely overestimates the rate constant. Therefore one should reexamine interpretations of the slow fall–off behavior[9] which are based solely on the Grote–Hynes relation. Even though non-Markovian effects can influence the rate constant substantially it is not obvious if one can obtain order of magnitude enhancement for realistic potentials as predicted by the Grote–Hynes relation alone.

One has to be extremely careful not to draw any premature conclusions about the realistic case of several degrees of freedom from this study of a model with a single degree of freedom. Even though energy activation is much faster in the case of several degrees of freedom[23] it is not yet clear if effects as described here will be more or less important in these cases.

In the last few years it has become apparent that frequency dependent friction is only one of many possible explanations of the observed slow decrease of the rate constant as a function of viscosity. Recently it has been demonstrated on various systems that a simple equilibrium solvent effect can be the cause of such behavior.[24] It has also been shown that translational diffusion coefficients are often in substantial disagreement with the Stokes–Einstein relation exhibiting a fractional dependence on the viscosity η ($D \propto \eta^{-a}$ where $0 < a < 1$).[25] Finally, one might expect that a anisotropic friction in a system of several degrees of freedom can cause slow fall-off of the rate constant as a function of the damping.[26]

In conclusion we have used computer simulation to evaluate barrier crossing rate constants of a Brownian particle in a double well potential experiencing an exponential friction kernel. We find that for the large damping and long correlation times characteristic of many solvent systems the present theories grossly overestimate the rate constants for physically interesting barrier heights. For this reason we question the recent interpretations of chemical rate data which are based solely on the Grote–Hynes relation.

APPENDIX

Here we address briefly the problem of determining errors bars on calculated reactive fluxes. This method can be simply applied to obtain error bars from a single reactive flux. Recall that the reactive flux is obtained by averaging $\theta_A[x(t)]$ where $\theta_A(x)$ is the characteristic function which is 1 for reactants and 0 for products and x is the reaction coordinate. Suppose the reactive flux at time t is θ. An estimate of this quantity is obtained by computing the arithmetic mean $\bar{\theta}$ of N random variables which are either 1 with probability θ or 0 with probability 1-θ. The distribution function of $\bar{\theta}$ is binomial with a mean of θ and a variance $\theta(1-\theta)/N$ as shown in any statistics textbook.[27] The exact confidence intervals of $\bar{\theta}$ can be obtained from tables or scientific subroutine packages.[28] If N is large enough the binomial distribution approaches a normal distribution with the appropriate mean and variance for which the confidence intervals are easily obtained.

ACKNOWLEDGMENTS

We would like to thank P. Hänggi, P. Talkner, D. Thirumalai, D. Chandler for helpful discussions and J. T. Hynes for detailed and helpful comments on the manuscript.

[1]R. F. Grote and J. T. Hynes, J. Chem. Phys. **73**, 2715 (1980).
[2]R. F. Grote and J. T. Hynes, J. Chem. Phys. **77**, 3736 (1982); B. Carmeli and A. Nitzan, *ibid.* **79**, 393 (1983); R. Zwanzig, Phys. Fluids **2**, 12 (1959).
[3]P. Hänggi and F. Moitabai, Phys. Rev. A **26**, 1168 (1982); P. Hänggi, J. Stat Phys. **30**, 401 (1983); P. Hänggi and U. Weiss, Phys. Rev. A **29**, 2265 (1984).
[4]B. Carmeli and A. Nitzan, J. Chem. Phys. **80**, 3596 (1984); B. Carmeli and A. Nitzan, Phys. Rev. A **29**, 1481 (1984); A. Nitzan, J. Chem. Phys. **82**, 1614 (1985).
[5]P. Hänggi, J. Stat. Phys. **42**, 105 (1986).
[6]H. A. Kramers, Physica **7**, 284 (1940).
[7]B. J. Matkowski, Z. Schuss, and C. Tier, J. Stat. Phys. **35**, 443 (1984).
[8]T. Hasha, T. Eguchi, and J. Jonas, J. Am. Chem. Soc. **104**, 2290 (1982); M. Lee, G. R. Holton, and R. M. Hochstrasser, Chem. Phys. Lett. **118**, 359 (1985); G. Manecke, J. Schroeder, J. Troe, and F. Voss, Ber. Bunsenges. Phys. Chem. **89**, 896 (1985); B. Otto, J. Schroeder, and J. Troe, J. Chem. Phys. **81**, 202 (1984).
[9]B. Bagchi and D. W. Oxtoby, J. Chem. Phys. **78**, 2735 (1983); G. Rothenberger, D. K. Negus, and R. Hochstrasser, J. Chem. Phys. **78**, 249 (1983); K. Eisenthal, and A. Millar (preprint).
[10]A. G. Zawadski and J. T. Hynes, Chem. Phys. Lett. **113**, 476 (1985).
[11]J. E. Straub and B. J. Berne, J. Chem. Phys. **83**, 1138 (1985); J. E. Straub, D. A. Hsu, and B. J. Berne, J. Phys. Chem. **89**, 5188 (1985).
[12]J. E. Straub, M. Borkovec, and B. J. Berne, J. Chem. Phys. **83**, 3172 (1985).
[13]J. A. Montgomery, D. Chandler, and B. J. Berne, J. Chem. Phys. **70**, 4065 (1979).
[14]R. Zwanzig and M. Bixon, Phys. Rev. A **2**, 2005 (1970); H. Metiu, D. Oxtoby, and K. F. Freed, *ibid.* **15**, 361 (1977).
[15]J. L. Skinner and P. G. Wolynes, J. Chem. Phys. **72**, 4913 (1980).
[16]See, for example, C. W. Gardiner, *Handbook of Stochastic Methods* (Springer, New York, 1983).
[17]G. van der Zwan and J. T. Hynes, J. Chem. Phys. **76**, 2993 (1982). The case of our $\alpha^* < 1$ is referred to as "strong solvent forces" and $\alpha^* > 1$ as "weak solvent forces".
[18]M. Borkovec and B. J. Berne, J. Phys. Chem. **89**, 3994 (1985).
[19]See, for example, K. E. Atkinson, *An Introduction to Numerical Analysis* (Wiley, New York, 1978).
[20]F. Marchesoni and P. Grigolini, J. Chem. Phys. **78**, 6287 (1983).
[21]S. P. Velsko, D. H. Waldeck, and G. R. Fleming, J. Chem. Phys. **78**, 249 (1983).
[22]R. F. Grote and J. T. Hynes, J. Phys. Chem. **88**, 4676 (1984), and references therein.
[23]See, for example, M. Borkovec and B. J Berne, J. Chem. Phys. **82**, 794 (1985), and references therein.
[24]J. Hicks, M. Vandersall, and K. Eisenthal, Chem. Phys. Lett. **116**, 18 (1985); V. Sundstrom and T. Gillbro, Ber. Bunsenges. Phys. Chem. **89**, 222 (1985); J. Troe, Chem. Phys. Lett. **116**, 453 (1985).
[25]G. L. Pollack and J. J. Enyeart, Phys. Rev. A **31**, 980 (1985); H. J. V. Tyrrell and K. R. Harris, *Diffusion in Liquids* (Butterworths, London, 1984), Chap. 7.2.
[26]R. F. Grote and J. T. Hynes, J. Chem. Phys. **74**, 4465 (1981); **75**, 2191 (1981); G. van der Zwan and J. T. Hynes, *ibid.* **77**, 1295 (1977); Chem. Phys. **90**, 21 (1984); J. E. Straub and B. J. Berne (in preparation); G. R. Flemming (private communication).
[27]See, for example, R. W. Hogg and A. T. Craig, *Introduction to Mathematical Statistics* (Macmillan, New York, 1978), Chap. 3.
[28]See, for example, subroutine BELBIN in the IMSL-scientific subroutine package.

ERRATA

Erratum and addendum: Non-Markovian activated rate processes: Comparison of current theories with numerical simulation data [J. Chem. Phys. 84, 1788 (1986)]

John E. Straub, Michal Borkovec, and Bruce J. Berne
Department of Chemistry, Columbia University, New York, New York 10027

(Received 29 September 1986; accepted 29 September 1986)

There are several misprints. (1) ζ on the right-hand side of Eq. (3) should read γ. (2) In the caption of Fig. 1 ● and ○ should be interchanged. (3) On the right-hand side of Eq. (18), 1 should be replaced by 2. (4) The ordinate in Fig. 4(a) should be labeled from -2 to $+2$.

Let us clarify the units and the potential used in the simulation. We choose unit mass and unit barrier energy throughout. The symmetric parabolic potential reads for positive x:

$$U(x) = 1 - \frac{\omega_B^2}{2} x^2 \quad \text{for } x < x_1 ,$$

$$U(x) = \frac{\omega_0^2}{2} (x - x_0)^2 \quad \text{for } x > x_1 .$$

Continuity of the potential and force determines x_0 and x_1 by $x_0 = x_1[1 + (\omega_B/\omega_0)^2]$ and $x_1^2 \omega_B^2 [1 + (\omega_B/\omega_0)^2] = 2$. The thermal energy $k_B T$ is $1/(\beta Q)$ in these units. Actually, ω_B may also be set to one which adjusts the time unit to ω_B^{-1}. This gives rise to the reduced variables $\gamma^* = \gamma/\omega_B$ and $\alpha^* = \alpha \omega_B^2$.

 0021-9606/87/021079-01$02.10